MATHEMATICAL MODELING AND SIMULATION OF A LOW TEMPERATURE SOLAR THERMAL ENERGY CONVERSION SYSTEM

Situmbeko S.M., Inambao F.L.

University of KwaZulu-Natal, Durban (South Africa)

Abstract

Research and development work on Low Temperature Energy Conversion has great potential for harnessing waste heat and low energy density solar radiation. This has implications on improving plant thermal efficiencies and promoting recovery and utilization of waste energy otherwise conventionally regarded unusable. A low temperature solar thermal system typically uses flat plate and low concentrating collectors such as parabolic troughs. Such collectors are relatively simpler in construction, easier to operate owing to the absence of complex solar tracking equipment and therefore more suited to remote and rural outposts. Such systems operate within temperatures ranges below 300^{o}C. This calls for changes to the conventional conversion systems and necessitates substituting the heat transfer and working fluids; a subject currently invoking immense research interests. This paper presents a mathematical model based on such a concept plant. The mathematical model is developed from in-depth analyses of energy balances and thermo-fluid dynamics at component, subsystem and system levels. Simulations are carried out by employing a combination of various computer software's such as EEE (Engineering Equation Solver), F-chart and Polysun. Different configurations are considered by varying heat transfer fluids, working fluids and plant layouts. Results of the simulations are presented in the final paper. These results will inform the physical investigations that are to follow in the next stage of the research.

Keywords: Low temperature, energy conversion, solar thermal, heat transfer fluid, working fluid, mathematical model, simulation

1. Introduction

Solar energy technology has great potential but its full development is hampered by some major drawbacks. Solar energy conversion technologies have lower efficiencies and higher costs when compared with other energy sources and technologies; solar radiation has a relatively low energy density thus requiring large harvesting fields. Table 1 shows energy conversion efficiencies of some common conversion systems and the chart shows levelized electricity costs from different sources/ technologies.

Table 1. Energy Conversion Efficiencies [1]

Conversion Process – Electricity Generation	**Efficiency**
Gas turbine	up to 40%
Gas turbine plus steam turbine (combined cycle)	up to 60%
Water turbine	up to 90% (practically achieved)
Wind turbine	up to 59% (theoretical limit)
Solar cell	6%-40% (technology dependent, 15% most often, 85%-90% theoretical limit)
Fuel cell	up to 85%
*Solar – Thermal CSP	
*Solar – Thermal ORC	3 – 25 %

* added to table from other sources

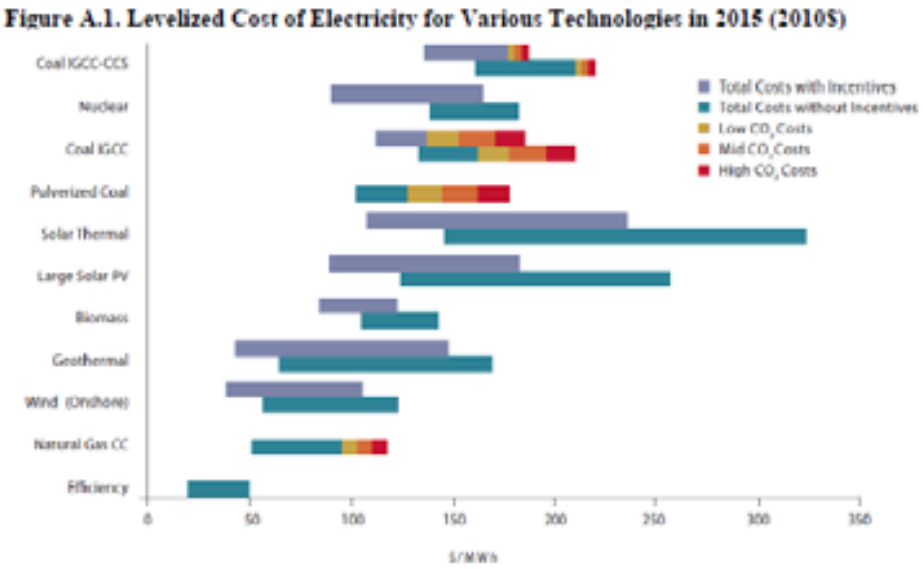

Figure 1. Levelized Cost of Electricity for Various Technologies [2]

The solar radiation measured just outside the earth's atmosphere, the solar constant, averages 1365 W/m^2. Ignoring clouds, the average insolation for the Earth is approximately 250 watts per square meter (6 (kW·h/m^2)/day), taking into account the lower radiation intensity in early morning and evening, and its near-absence at night. [3]

Solar energy technologies include moderate temperature systems for space heating (including swimming pool and domestic hot water), moderate to high temperatures for industrial processes, high temperature for electricity generation (commonly referred to as Concentrated Solar Power), Photovoltaic and Oceanic Thermal Energy Conversion for electricity generation.

So if we can avoid high costs by developing simple conversion devices with minimum number of components and still be able to harness this low energy density resource the technology potential might have a prospect of improvement. Researchers and developers of ORC generally agree on the need to maintaining simplicity and low cost through keeping the number of plant devices few. Low temperature operation allows cheaper and safer operating conditions; thus adoption of a single stage small (micro) expander removes the usual complexity associated with conventional power plants. Another plus to this technology is that if adopted for harnessing waste heat it still has an infinitesimal incremental effect onto the overall plant energy efficiency with considerably lower associated cost increase.

This paper proposes an appropriate mathematical modeling and computer simulation scheme for a low temperature solar thermal energy conversion system. The analysis covers a wide range of candidate working fluids and different optimal cycle configurations. The results of this model will be incorporated in a physical model to be build and validated as part of the ongoing research.

2. First Pass Mathematical Modeling

The modeling has been done in two parts; the first part, which is presented in this section, being the first pass model gives an initial insight into the performance of the proposed energy conversion system design. The output of this first model forms an input into the second part, the detailed model, not included in this paper. This first pass model output together with the more detailed specifications of components for the proposed system design will yield a

more detailed model with more realistic performance parameters that can now be incorporated in the design, development and validation of the physical model.

In this work a more generalized model is first proposed. This is then further customized to the thermo-physical properties of the different proposed working fluids. In particular a mathematical logic model is incorporated to assign an appropriate cycle configuration to each proposed working fluid.

2.1 Thermal Cycle

The first pass model serves to provide a first performance indicator which can then be improved in subsequent models as more details of the system, subsystems and components are generated.

The first pass model makes a number of assumptions such as:

- the pumping and expansion are adiabatic
- the thermal losses in the cycle components and ducting are negligible.
- the pressure head losses in the heat exchangers are negligible.
- no work and no heat transfer occurs in the valves, etc.

Three types of models can be identified with low temperature thermal cycles depending on the nature of the working fluid. Based on the fluids' T-s saturation curves these three types of energy conversion systems are: the conventional rankine cycle, the rankine cycle with a recuperator and the rankine cycle with a superheater. In order to develop a generalized model that can be simulated using a computer program, a general configuration is indicated here from which the three models will be generated.

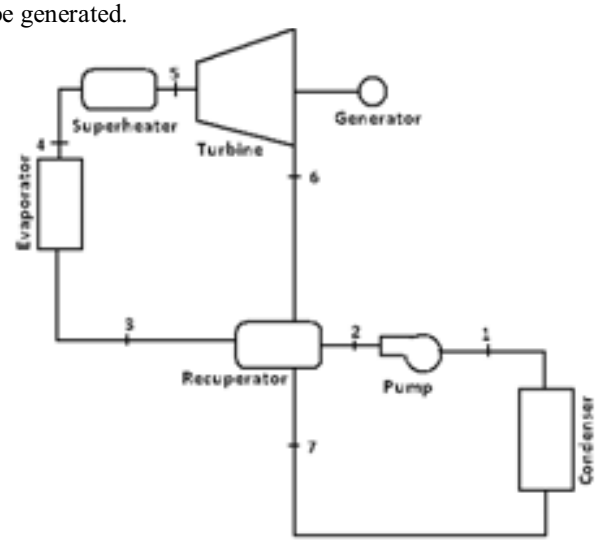

Figure 2. General Configuration of the Organic Rankine Cycle

In order to come up with any of the three configurations the two states representing the input and output of any device that is to be excluded in the model are merged as shown in figure 3.

Description of T-s curve	T-s curve Diagram	Recommended Cycle configuration
Isentropic Vapour Saturation Curve	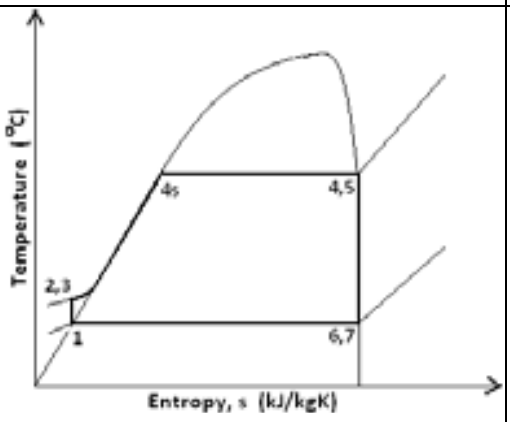	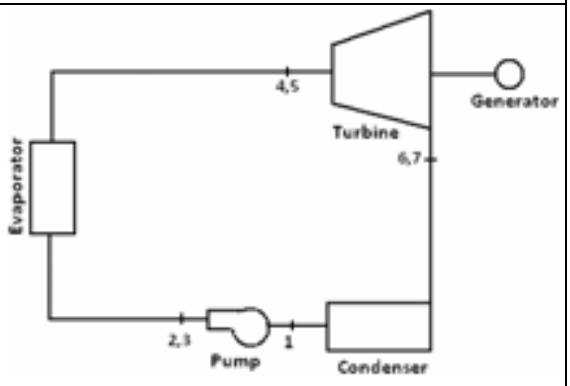 Model 1: Conventional Rankine
Positive Vapour Saturation Curve	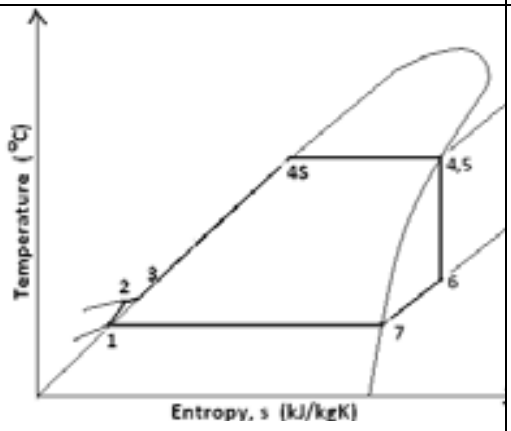	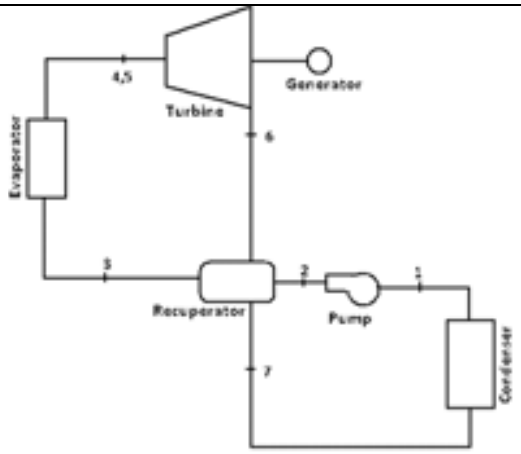 Model 2: Rankine with Recuperator
Negative Vapour Saturation Curve	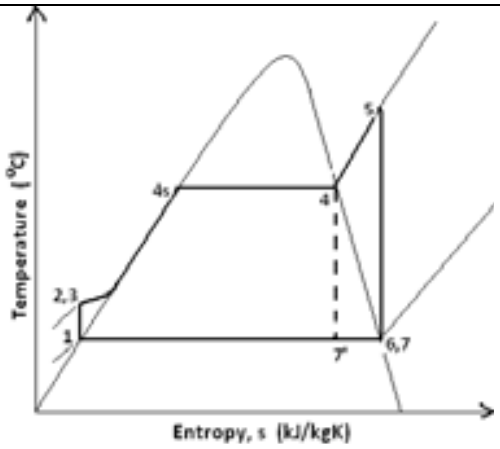	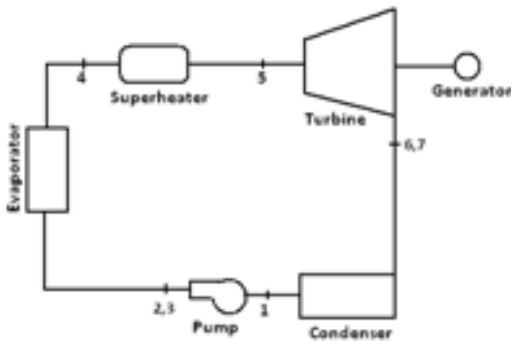 Model 3: Rankine with Superheater

Figure 3. Different Model Configurations of the Organic Rankine Cycle

2.1.1 Isentropic Vapour Saturation Curve

With the Isentropic saturation curve the process diagram includes only the turbine, pump, evaporator and condenser. The vapour remains a saturated vapour during expansion process from the higher temperature and higher pressure at the turbine entry to the lower temperature and lower pressure at the turbine exit; there is no risk of damage to the turbine blades due to formation of liquid droplets and there is no excessive residual heat in the vapour at the turbine exhaust.

The four processes making up the thermal energy conversion cycle and identified by numbers in the cycle diagram are:

Process 1-2: The working fluid is pumped from low to high pressure, as the fluid is a liquid at this stage the pump requires little input energy.
Process 3-4: The high pressure liquid enters a boiler where it is heated at constant pressure by an external heat source to become a dry saturated vapor. Note that states 2 and 3 are merged as there is no recuperating device.
Process 5-6: The dry saturated vapor expands through a turbine, generating power. This decreases the temperature and pressure of the vapor. Note also here, that states 4 and 5 are merged as there is no superheating device.
Process 7-1: The dry saturated turbine exhaust vapor then enters a condenser where it is condensed at a constant pressure and temperature to become a saturated liquid. The pressure and temperature of the condenser is fixed by the temperature of the cooling coils as the fluid is undergoing a phase-change. States 6 and 7 coincide due to the absence of a recuperator.

The mathematical models for the four processes are derived from the energy and mass balance for a control volume.

Pump: $$\frac{\dot{W}_{pump}}{\dot{m}} = (h_2 - h_1) \approx \frac{v_1 \Delta P}{\eta_{pump}} \approx \frac{P_2 - P_1}{\eta_{pump}} \quad (2.1)$$

Turbine: $$\frac{\dot{W}_{turbine}}{\dot{m}} = (h_5 - h_6) = (h_5 - h_{6s}) \times \eta_{turbine} \quad (2.2)$$

In a real Rankine cycle, the compression by the pump and the expansion in the turbine are not isentropic. In other words, these processes are non-reversible and entropy is increased during the two processes. This increases the power required by the pump and decreases the power generated by the turbine. The models take this into account by incorporating the isentropic efficiencies.

Evaporator: $$\frac{\dot{Q}_{evap}}{\dot{m}} = (h_4 - h_3) \quad (2.3)$$

Condenser: $$\frac{\dot{Q}_{cond}}{\dot{m}} = (h_7 - h_1) \quad (2.4)$$

2.1.2 Positive Vapour Saturation Curve

In some cases, the vapour exiting the turbine attains the lower pressure in a superheated state. This imposes a larger cooling load on the condenser and consequently reduces the cycle thermal efficiency. In order to overcome this a recuperator is added to the system to provide preheating through heat exchange between the vapor exiting the turbine and the working fluid before in enters the evaporator and thus reduce the cooling load on the condenser as well as the heating load on the evaporator. The recuperator is applicable when the organic fluid is of the "dry expansion" type, namely a fluid where the expansion in the turbine is done in the dry superheated zone and the expanded vapor contains heat that has to be extracted prior to the condensing stage. The recuperated Organic Rankine cycle is typically 10-15% more efficient than the simple Organic Rankine cycle.

In addition to the four processes of the Isentropic Saturation Curve we now have two additional processes taking place in the Recuperator as follows:

Process 2-3: The high pressure working liquid from the pump is preheated in the recuperator to a higher temperature before it enters the evaporator.

Process 6-7: The superheated low pressure dry vapor exiting the turbine enters a recuperator where it loses some heat at constant pressure to become a saturated dry vapour before entering the condenser.

Recuperator – Cold Stream: $$\frac{\dot{Q}_{recu}}{\dot{m}} = (h_3 - h_2) \quad (2.5)$$

Recuperator – Hot Stream: $$\frac{\dot{Q}_{recu}}{\dot{m}} = (h_6 - h_7) \quad (2.6)$$

2.1.3 Negative Vapour Saturation Curve

These types of organic fluids are referred to as "wet" or as having a negative Isentropic Vapour saturation curve; these liquids resemble much the curve for water. If the working fluid is fed into the turbine in a dry saturated state, it ends as a mixture of liquid and vapour upon expansion. This is undesirable as the formation of liquid droplets tend to cause pitting erosion on the turbine blades and gradually reduce the efficiency of the turbine. This problem is overcome by superheating the vapour before it enters the turbine so that it ends in a dry saturated vapour after expansion.

Thus in addition to the four processes of the Isentropic Saturation Curve we now have one additional process taking place in the Superheater:

Process 4-5: The high pressure dry saturated vapour from the evaporator is further heated at constant pressure in the superheater to a higher temperature superheated state. The superheated state is designed to coincide with the end state after expansion resulting in a dry saturated state at the lower pressure assuming ideal (isentropic) expansion.

Superheater: $$\frac{\dot{Q}_{superheater}}{\dot{m}} = (h_5 - h_4) \quad (2.7)$$

The reason for assuming a dry saturated end state under isentropic expansion is that due to the fact that at this state the performance of the superheater is not yet ascertained (will also deteriorate with operation) and that it is safer to assume it lower, fixing the real end state at dry saturated state risks ending the expansion in a wet state.

The final equation in the thermal model defines the thermodynamic efficiency of the cycle as the ratio of net power output to heat input. As the work required by the pump is often around 1% of the turbine work output, equation 5 can be simplified.

Thermal efficiency: $$\eta_{therm} = \frac{\dot{W}_{turbine} - \dot{W}_{pump}}{\dot{Q}_{in}} \approx \frac{\dot{W}_{turbine}}{\dot{Q}_{in}} \quad (2.8)$$

Where $\dot{Q}_{in}$is defined as $\dot{Q}_{in} = \dot{Q}_{evap} + \dot{Q}_{superheater}$ and in cases where there is no superheating as simply $\dot{Q}_{in} = \dot{Q}_{evap}$

2.2 Solar Cycle

The first pass mathematical model of the solar thermal cycle is governed by the Hottel-Whillier equation. [4]

$$Q_u = A_C F_R [\tau\alpha G - U(T_{in} - T_a)] \quad (2.9)$$

where A_C (m^2) is the solar collector field aperture area, F_R is the heat removal factor, τ is the cover glazing transmittance, α is the absorber absorptance and U is the overall heat loss coefficient of the solar collector field. Operational conditions are solar insolation G, heat transfer fluid inlet temperature T_{in} and ambient temperatureT_a.

2.3 Model Type Selection

This is incorporated by first selecting an acceptable difference between the entropy values of the working fluid dry saturated vapour at the lower and higher pressures that would be considered as Isentropic. The model then proceeds, for all cases not satisfying this requirement, to determine which entropy is larger; if the lower pressure entropy is larger the working fluid falls into the negative vapour saturation curve and if the higher pressure entropy is larger, the positive vapour saturation curve. Mathematically the model selection is expressed as:

$$If \ \frac{[s_{high}-s_{low}]}{s_{low}} < \delta \ \ then \ Isentropic \ Curve \ Model \ is \ selected \tag{2.10}$$

Otherwise

$$If \ s_{high} > s_{low} \ , Positive \ Saturation \ Curve \ Model \ is \ selected \ or \tag{2.11}$$

$$If \ s_{low} > s_{high} \ , Negative \ Saturation \ Curve \ Model \ is \ selected$$

3. Computer Simulation

Engineering Equation Solver (EES) software is used to develop the computer simulation code. The EES code consists of the Solar Model and Model Selection Procedures in addition to the main Thermal Model code.

A lookup table listing the working fluids to be analysed is called up during the running of the code. A parametric table is included to define the type of output data required.

EES software has inbuilt thermophysical properties of several working fluids as well as other materials. It also allows the user to incorporate properties of materials not included in the initial software.

4. Results

The results from the computer simulations are shown in tables 2 and 3 appended to this paper. The results shown here do not include the Solar Model code which is yet to be incorporated.

6. Conclusion

Fourteen working fluids have been tested with the model. The model assigned six working fluids (Benzene, n-butane, Isobutane, R141b, R245fa, R123) to Model 1, Conventional Rankine, five working fluids (n-pentane, n-hexane, Isopentane, R113, Toluene) to Model 2, Rankine with Recuperator, and three working fluids (R22, R134a, Water) to Model 3, Rankine with Superheater. Water is included as a control since it is well established that water requires superheating. The thermal efficiencies vary from 10.38% for R245fa (Conventional Rankine) to 12.04% for n-pentane (Rankine with Recuperator). The model requires further improvement to include error reporting for results that are outside the feasible solutions. Particularly, with heat exchangers, the working fluid may not attain certain temperatures with low temperatures energy sources. For instance the high pressure temperatures reported for certain working fluids such as 271.8^{o}C for water, 178.3^{o}C for Toluene, 142.7^{o}C for Benzene and 131.3^{o}C for n-hexane may not be feasible with flat plate collectors.

In concluding, the mathematical model was successfully developed into EES code and computer simulations conducted with fourteen different working fluids. Three models were developed to optimize the energy cycle performance based on thermodynamic properties of the working fluids. These models will be further developed into detailed models. The results will be presented in future reports. This model has shown that low temperature solar thermal energy conversion is feasible and potential for further development.

7. References

[1] http://en.wikipedia.org/wiki/Energy_conversion_efficiency accessed August 14, 2011
[2]http://www.ucsusa.org/assets/documents/clean_energy/Appendix-Key-Assumptions-Levelized-Costs.pdf accessed August 10, 2011.
[3] http://en.wikipedia.org/wiki/Insolation accessed August 10, 2011
[4]Duffie J.A., Beckman W.A., "Solar Engineering of Thermal Processes" 2nd Ed., John Wiley & Son, Inc., USA, 1991 ISBN 0-471-51056-4 p281
[5] Engineering Equation Solver (EES) software

Table 2. Thermal Efficiencies of Different Organic Rankine Cycle Configurations and Different Working Fluids

Model Type	Working Fluid	Q_dot_ evaporator	Q_dot_ recuperator	Q_dot_ superheater	Power	eta_therm	s_high_s	s_low_s
		[kW]	[kW]	[kW]	[kW]	[%]	[kJ/kg.K]	[kJ/kg.K]
Rankine with Recuperator No Superheater	n-pentane	4.067	0.4041	0	0.4997	12.04	1.334	1.235
Conventional Rankine No Recuperator No Superheater	Benzene	4.68	0	0	0.5272	11.11	1.151	1.12
Conventional Rankine No Recuperator No Superheater	n-butane	4.558	0	0	0.539	11.6	2.439	2.408
Rankine with Recuperator No Superheater	n-hexane	3.753	0.6134	0	0.4641	12.1	1.44	1.29
Conventional Rankine No Recuperator No Superheater	Isobutane	4.306	0	0	0.5151	11.72	2.321	2.3
Conventional Rankine No Recuperator No Superheater	R141b	2.6	0	0	0.2987	11.3	1.019	1.013
Rankine with Recuperator No Superheater	Isopentane	3.901	0.376	0	0.4859	12.2	-0.4366	-0.5304
Conventional Rankine No Recuperator No Superheater	R245fa	2.301	0	0	0.2432	10.38	1.77	1.75
Rankine with Recuperator No Superheater	R113	1.64	0.156	0	0.1991	11.89	0.7684	0.7317
Conventional Rankine No Recuperator No Superheater	R123	2.021	0	0	0.2268	11.02	1.685	1.668
Rankine with Superheater No Recuperator	R22	2.496	0	0.2123	0.3296	12.01	1.751	1.825
Rankine with Recuperator No Superheater	Toluene	4.094	0.4495	0	0.489	11.75	1.032	0.9404
Rankine with Superheater No Recuperator	R134a	2.413	0	0.08032	0.2784	10.99	0.9242	0.9516
Rankine with Superheater No Recuperator	Water	23.29	0	2.569	2.803	10.81	6.822	7.355

Table 3. Other Parameters for Different Organic Rankine Cycle Configurations and Different Working Fluids

Working Fluid	T[1]	T[2]	T[3]	T[4]	T[5]	T[6]	T[7]	h[1]	h[2]	h[3]	h[4]	h[5]	h[6]	h[7]
	[C]	[C]	[C]	[C]	[C]	[C]	[C]	[kJ/kg]	[kJ/kg]	[kJ/kg]	[kJ/kg]	[kJ/kg]	[kJ/kg]	[kJ/kg]
n-pentane	35.87	36.17	52.94	92.74	92.74	58.26	35.87	23.38	24.39	64.8	471.5	471.5	421.5	381.1
Benzene	80.07	80.33	80.33	142.7	142.7	96.87	96.87	3E-05	0.7541	0.7541	468.7	468.7	416	416
n-butane	-0.521	-0.133	-0.133	50.26	50.26	10.38	10.38	199	200	200	655.8	655.8	601.9	601.9
n-hexane	69.28	69.58	94.75	131.3	131.3	100.5	69.28	104.5	105.5	166.8	542.2	542.2	495.8	434.4
Isobutane	-11.67	-11.25	-11.25	37.74	37.74	-2.53	-2.53	173.7	174.8	174.8	605.3	605.3	553.8	553.8
R141b	32.07	32.5	32.5	86.89	86.89	41.03	41.03	75.69	76.19	76.19	336.1	336.1	306.3	306.3
Isopentane	27.86	28.16	44.35	83.77	83.77	49.15	27.86	-343.5	-342.5	-304.9	85.18	85.18	36.59	-1.005
R245fa	15.19	15.43	15.43	62.79	62.85	26.24	26.24	219.6	220	220	450.1	450.1	425.8	425.8
R113	47.61	48.04	64.22	105.7	105.7	69.54	47.61	77.59	77.99	93.6	257.6	257.6	237.7	222.1
R123	27.79	28.11	28.11	80.82	80.82	40.66	40.66	229.1	229.5	229.5	431.6	431.6	408.9	408.9
R22	-40.81	-39.14	-39.14	0.1148	29.52	-31.19	-31.19	155.2	155.6	155.6	405.2	426.5	393.5	393.5
Toluene	110.4	110.6	132.6	178.3	178.3	139.8	110.4	-0.425	0.3616	45.31	454.7	454.7	405.8	360.9
R134a	-26.09	-25.87	-25.87	15.71	24.08	-19.9	-19.9	17.63	18.08	18.08	259.4	267.4	239.6	239.6
Water	99.97	100.1	100.1	151.8	271.8	124.5	124.5	419	419.6	419.6	2749	3005	2725	2725

Table 3. continued

Working Fluid	s[1]	s[2]	s[3]	s[4]	s[5]	s[6]	s[7]
	[kJ/kg·K]	[kJ/kg·K]	[kJ/kg·K]	[kJ/kg·K]	[kJ/kg·K]	[kJ/kg·K]	[kJ/kg·K]
n-pentane	0.07778	0.07892	0.2061	1.334	1.334	1.361	1.235
Benzene	1.09E-07	0.000747	0.000747	1.151	1.151	1.176	1.176
n-butane	0.9964	0.9977	0.9977	2.439	2.439	2.473	2.473
n-hexane	0.3267	0.3278	0.5004	1.44	1.44	1.462	1.29
Isobutane	0.9021	0.9035	0.9035	2.321	2.321	2.355	2.355
R141b	0.2812	0.2828	0.2828	1.019	1.019	1.036	1.036
Isopentane	-1.668	-1.667	-1.546	-0.4366	-0.4366	-0.4098	-0.5304
R245fa	1.07	1.07	1.07	1.77	1.77	1.784	1.784
R113	0.2813	0.2826	0.3298	0.7684	0.7684	0.7788	0.7317
R123	1.101	1.102	1.102	1.685	1.685	1.698	1.698
R22	0.8241	0.8248	0.8248	1.751	1.825	1.849	1.849
Toluene	-0.00111	-0.00039	0.1135	1.032	1.032	1.053	0.9404
R134a	0.07331	0.07394	0.07394	0.9242	0.9516	0.9712	0.9712
Water	1.307	1.307	1.307	6.822	7.355	7.483	7.483